Journal of the Korean Physical Society, Vol. 61, No. 7, October 2012, pp. 1108∼1113

Rheological Correlations of Relaxation Time for Finite Concentrated Semiflexible Polyelectrolytes in Solvents

Myung-Suk Chun*
Complex Fluids Laboratory, National Agenda Research Division, Korea Institute of Science and Technology (KIST), Seoul 136-791, Korea

Min Jae Ko
Photo-Electronic Hybrids Research Center, Korea Institute of Science and Technology (KIST), Seoul 136-791, Korea

(Received 17 August 2012, in final form 27 August 2012)

The Rouse-Zimm model based on the polymer dynamics theory allows us to predict the relaxation time of polyelectrolyte dilute solution as a function of the intrinsic viscosity. In finite concentrated solutions, the empirical analysis adopted in this study is quite useful to examine the relaxation behavior, noting that proper theories are not well-clarified and experimental measurements are rather complicated. For the xanthan biopolymer selected as the polyelectrolyte model of a semiflexible chain, we measured rheological properties of shear viscosity η and first normal stress difference $\sigma_{\Delta 1}$ in dilute and semidilute solutions over a wide range of shear rates $\dot{\gamma}$. Power-law scaling relations are commonly observed in the region of $\dot{\gamma} \geq 1\ \mathrm{s}^{-1}$. Accurate regressions on η and $\sigma_{\Delta 1}$ present empirical plots as functions of the shear rate and the xanthan concentration, from which each of relevant fitting parameters are determined. Empirically determined curves agree well with the experimental data, ensuring that the empirical formula for the characteristic relaxation time λ is applicable at dilute and finite concentrations, which has not been reported in the literature. We further interpreted the non-Newtonian fluid behavior over a full range of shear rates by applying the Carreau A constitutive model.

PACS numbers: 83.60.Fg, 83.85.Cg, 82.35.Rs, 83.85.Ns
Keywords: Polyelectrolyte, Rheology, Relaxation time, Shear viscosity, Normal stress, Polymer physics
DOI: 10.3938/jkps.61.1108

I. INTRODUCTION

Polyelectrolytes, or charged polymers, include many proteins and other biopolymers, such as DNA and polysaccharides. A polyelectrolyte in solvents is a kind of typical complex fluid, representing an interesting and broad class of soft matter [1–3]. Due to its fascinating conformational change in an aqueous medium that is a poor solvent for most synthetic polymers, many reliable theories developed for neutral polymers cannot be applied directly [4]. Usually, it is necessary to consider more system-specific aspects represented by the surface charge, relaxation, and counterion condensation [5].

The relaxation of polymer chains, which is of fundamental importance in studying the dynamic and the rheological behaviors of polyelectrolyte soft matter, can be generally understood as the product of competing elasticity and hydrodynamic drag. A precise understanding of the relaxation dynamics of soft matter in confined spaces is receiving increasing attention [6–8]. In particular, it is important in many biophysical applications, for instance, DNA sequencing and gene mapping by using micro/nanofluidic lab-on-chips [9–11]. The relaxation time of polyelectrolyte chains means how fast it recovers from its deformation or stress. In the Maxwell model, the relaxation time is defined by the ratio of the viscosity of the viscous element to the modulus of the elastic element. The generalized Maxwell model may have a finite number of different Maxwell relaxation times, leading to different moduli of the chain [12]. According to molecular theory, characteristic relaxation time λ of polyelectrolyte chains in solvents is given by the sum over the spectrum of the relaxation times, $\lambda = \Sigma\ \lambda_i$. From rheological data at steady shear, λ for finite concentrated polyelectrolytes is approximately obtained by the ratio of the first (or primary) normal stress difference $\sigma_{\Delta 1}$ to the product of the shear rate $\dot{\gamma}$ and the shear stress τ [13]

$$\lambda \simeq \frac{1}{2}\frac{\sigma_{\Delta 1}}{\dot{\gamma}\tau} \equiv \frac{1}{2}\frac{\sigma_{\Delta 1}}{\eta\dot{\gamma}^2}. \quad (1)$$

Here, note that the normal stress difference is physically

*E-mail: mschun@kist.re.kr; Tel: 82-2-958-5363; Fax: 82-2-958-5205

associated with nonlinear effects, and η $(=\dot{\gamma}/\tau)$ is the shear viscosity.

Basically, dynamics of polymer chains are modeled by Rouse theory [14] and Zimm theory [15]. Rouse theory can explain the polymer dynamics of a freely draining Gaussian chain. Zimm theory considers hydrodynamic interactions between the bead segment and the solvent by using bead-spring model. Relaxation properties of a semiflexible or wormlike polyelectrolyte polymer in solvents have been investigated by employing either computations or experiments [16–20]. The model polyelectrolytes in previous studies were almost always confined to a DNA molecule with a contour length of above several micrometers. The longest relaxation time scaled as molecular length $L^{1.65}$ shows an agreement with the dynamic scaling predictions of the Zimm model [16].

There are very few studies to readily predict the relaxation time for a wide range of the polymer concentration, noting that the available explanations and results are sometimes conflicting. In this regard, a main thrust of the present paper is to develop an empirical analysis for polyelectrolyte solutions connecting between theory and experiments. From the rheological data and the viscometric functions of η and $\sigma_{\Delta 1}$, we examine the empirical correlation for the relaxation of xanthan biopolymer, which is taken as a model polyelectrolyte, as functions of shear rate and concentration. This can serve as an extended work for further understanding the relaxation dynamics of submicron-sized semiflexible polyelectrolytes in solvents, which has not been attempted until now.

II. REVISITING THE ROUSE-ZIMM MODEL OF RELAXATION TIME IN DILUTE SOLUTION

Both the Rouse and the Zimm models predict the relaxation time of a polymer chain in either a theta or a good solvent for the case of dilute solution. The longest relaxation time λ_l can be defined by the ratio of the drag coefficient to the spring constant of the first normal coordinate. One can choose simply λ_l as the characteristic relaxation time λ, where λ_l equals to the longest rotational relaxation time and is twice the longest stress relaxation time. Here, we briefly describe on the models, because details are presented in the literature [12,13].

Figure 1 represents the basic concept of the polymer chain, which is also applicable to the polyelectrolyte. As a consequence of the Rouse model for the dynamics of dilute polymer solutions, the time correlation function provides the local motion of a polymer chain consisting of N links (or segments) with an effective bond length b [14]. It leads to the characteristic relaxation time as

$$\lambda^R = \frac{\xi (Nb)^2}{3\pi^2 k_B T}, \tag{2}$$

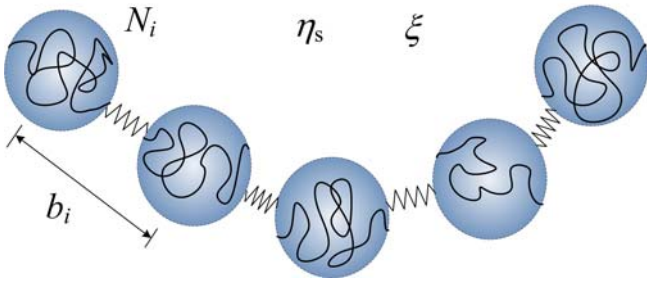

Fig. 1. (Color online) Illustration of the polyelectrolyte chain model with N segments and $N-1$ springs.

where ξ is the friction constant (*cf.*, $1/\xi$ is the mobility) and k_BT is the Boltzmann thermal energy. The intrinsic viscosity $[\eta]$ for polymer chains with molecular weight M_w in solvent viscosity η_s is calculated from the stress tensor in normal coordinates for each of independent mode p [12]. Adopting the Riemann zeta function $\sum_{p=1}^{\infty} p^{-s}$ [21], we reach

$$[\eta] = \frac{N_A}{M_w \eta_s} \frac{N^2 b^2 \xi}{6\pi^2} \sum_{p=1}^{\infty} p^{-2} = \frac{N_A}{M_w \eta_s} \frac{N^2 b^2 \xi}{36}, \tag{3}$$

where N_A is the Avogadro number. From Eq. (3), one obtains $(Nb)^2 = 36[\eta] M_w \eta_s / N_A \xi$. Now, the characteristic relaxation time is given by

$$\lambda^R = \frac{12}{\pi^2} \frac{\eta_s [\eta] M_w}{N_A k_B T}. \tag{4}$$

For the Zimm model in theta solvent, the hydrodynamic interaction is taken into account by the preaveraging approximation with Gaussian distribution of segment positions [12,15]. Although detailed procedures are not provided here, the characteristic relaxation time and the intrinsic viscosity are derived by

$$\lambda^Z = \frac{\eta_s (\sqrt{N} b)^3}{\sqrt{3\pi} k_B T}, \tag{5}$$

$$[\eta] = \frac{N_A (\sqrt{N} b)^3}{M_w \sqrt{3\pi}} \sum_{p=1}^{\infty} p^{-1.5} = 0.425 \frac{N_A (\sqrt{N} b)^3}{M_w}, \tag{6}$$

where $\sqrt{N} b$ corresponds to a root of the mean square of the end-to-end distance determined by each position of the first and the last beads. Getting $(\sqrt{N} b)^3 = [\eta] M_w / 0.425 N_A$ from Eq. (6) provides the characteristic relaxation time as

$$\lambda^Z = 0.766 \frac{\eta_s [\eta] M_w}{N_A k_B T}. \tag{7}$$

The Zimm model in good solvent includes the excluded volume effect in the distribution of the chain segments [12,13]. By applying the linearization approximation to

the distribution, we have

$$\lambda^Z = \frac{\eta_s (N^\nu b)^3}{k_B T}, \quad (8)$$

$$[\eta] \cong \frac{N_A N^{3\nu}}{M_w} \sum_{p=1}^{\infty} p^{-3\nu} b^3 \simeq \frac{N_A}{M_w} (N^\nu b)^3. \quad (9)$$

Equation (9) is rewritten as $(N^\nu b)^3 \cong [\eta] M_w / N_A$, where $N^\nu b$ is equivalent to the radius of gyration R_G of the polymer chain. Then, the characteristic relaxation time is given by

$$\lambda^Z \cong \frac{\eta_s [\eta] M_w}{N_A k_B T}. \quad (10)$$

Note that the Zimm model predicts that the relaxation of a chain would exhibit modes with time constants scaling as a power of the contour length R_C of the polymer, where $R_C = (N-1)b = \sum_{i=1}^{N-1} b_i$.

In the case of a dilute polymer solution, the shear rate dependence of the relaxation time is possibly predicted by considering the shear rate dependence of the intrinsic viscosity. For a dilute polymer solution and at low shear rate, the shear rate dependence of $[\eta]$ is given as [22]

$$\frac{[\eta]}{[\eta]_0} = \frac{1}{1 + \beta(\lambda_T \dot{\gamma})^2}. \quad (11)$$

Here, $[\eta]_0$ is the zero-shear-rate (*i.e.*, Newtonian) intrinsic viscosity, β the empirical parameter, and λ_T the empirical time constant. For a finite concentration C_p of the polymer solution, $[\eta]$ can be replaced by $\lim_{C_p \to 0}[(\eta_o - \eta_s)/\eta_s C_p]$, where η_0 is the solution viscosity in the Newtonian regime.

III. RHEOLOGICAL CORRELATIONS

1. Semiflexible Polyelectrolyte Model

Xanthan, selected as the model polyelectrolyte, is an extracellular polysaccharide produced by bacterium. Its primary structure consists of a main chain with charged trisaccharide sidechains on every second residue and the side chain. Native xanthan is generally believed to exist in a double strand [23,24]. Depending on the conditions of temperature and salinity, its secondary structure is known to undergo an order-disorder (*i.e.*, helix-coil) transition. At low ionic strength of the solution, the extension of xanthan and the corresponding increase in the solution viscosity are likely to involve a transition of the secondary structure from a double strand to a disordered form, revealing denatured xanthan. Adding the salt results in the polyelectrolyte chain being screened by oppositely charged salt ions, becoming a collapsed state from an extended one. The powdered xanthan was purchased from Sigma Chemical Co. (St. Louis, MO). Special care was taken during sample preparation to remove microgels, and the solutions containing nearly monodisperse samples (*i.e.*, polydispersity ≤ 1.4) were obtained by employing membrane filtrations. The average molecular weight M_W of the native xanthan is 1.13×10^6 g/mol (approximately 1220 monomers), as determined by adopting the viscometric method [4,25].

The shear viscosity was measured at different xanthan concentrations C_p ranging from 0.005 wt% to 0.1 wt% by using a rotational rheometer (AR2000ex, TA Instruments, DE) with bob-and-cup fixtures. Here, 1 wt% is equivalent to 10^4 μg/ml or 10^4 ppm. Information for the primary normal stress $\sigma_{\Delta 1}$ behavior of xanthan is not available in the literature, so we measured $\sigma_{\Delta 1}$ for $0.018 \leq C_p$ (wt%) ≤ 0.18 by using another rheometer (ARES-LS, TA Instruments, DE) with a cone-and-plate geometry with a cone angle of 1° and a rebalance transducer.

Figures 2(a) and 2(b) present log-log plots, where all data were obtained at room temperature (25 °C) controlled within ±0.1 °C. The C_p variations are nearly identified as the region from dilute to semidilute concentration. In order to exclude complications arising from the long-range electrostatic interaction between monomers, xanthan polyelectrolyte is dispersed in aqueous solutions at a constant electrolyte concentration of 0.1-mM NaCl at a fixed pH. At this screening condition, R_G, R_C, and the persistence length l_P (*cf.*, statistical Kuhn length: $2l_P$) have about 213 nm, 960 nm, and 240 nm, respectively, ensuring a semiflexible wormlike chain as $R_C/l_P \geq 4$. Detailed information is presented in the previous study [25]. The data for $\sigma_{\Delta 1}$ in the range of either $\dot{\gamma} < 1$ s^{-1} or $C_p < 0.18$ wt% cannot be included because stable values are very difficult to obtain in those regions. Xanthan solution shows a typical non-Newtonian character of the pseudoplasticity yielding an inelastic fluid, where a zero-shear-rate plateau is observed [26]. The data reported here are the averages of three replicate data sets.

2. Empirical Analysis of Viscometric Functions

It is necessary that the rheological information should be determined as a function of both the shear rate and the polyelectrolyte concentration. In Fig. 2(a), shear thinning behavior is well illustrated for $\dot{\gamma} \geq 1$ s^{-1}. The shear viscosity has a constitutive relationship to obey a power-law model as

$$\eta(\dot{\gamma}, C_p) = K_n \dot{\gamma}^{n-1}, \quad (12)$$

where both parameters of the consistency K_n and the power-law exponent n for η scaling are functions of the xanthan concentration C_p in percent by weight (wt%). Figure 2(b) shows that the first normal stress difference $\sigma_{\Delta 1}$ increases with increasing $\dot{\gamma}$ for various xanthan concentrations, but the available $\dot{\gamma}$ region to get valid data becomes restricted with decreasing C_p. All data show

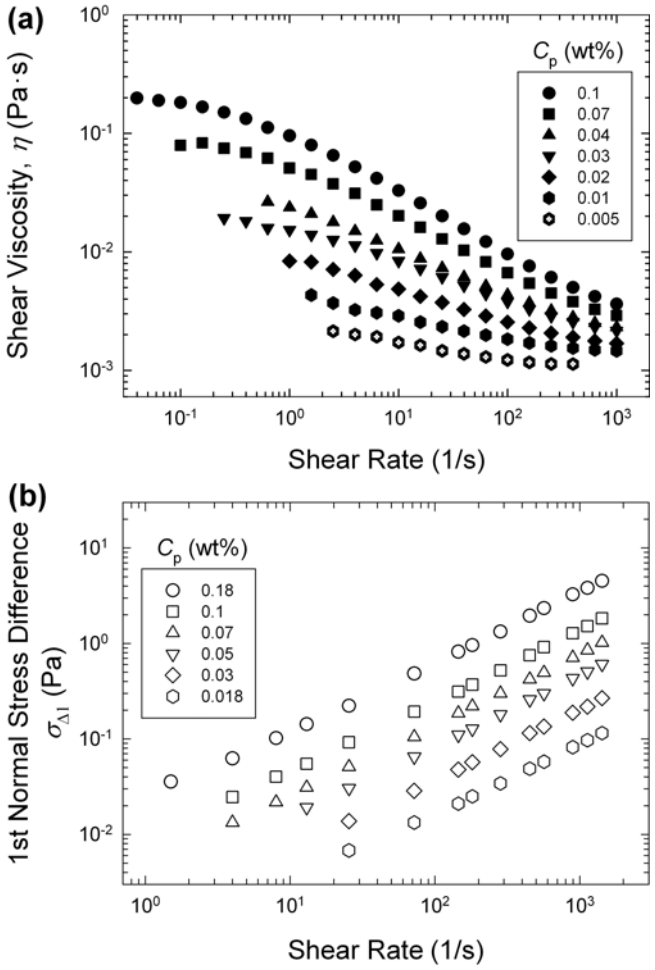

Fig. 2. Rheological data of (a) shear viscosity η and (b) first normal stress difference $\sigma_{\Delta 1}$ as functions of shear rate $\dot{\gamma}$ and xanthan polyelectrolyte concentration C_p at room temperature.

positive values of $\sigma_{\Delta 1}$ for all $\dot{\gamma}$. Considering experimental limits, one can suggest the scaling relations for $\dot{\gamma} > 1\ \mathrm{s}^{-1}$ as

$$\sigma_{\Delta 1}(\dot{\gamma}, C_p) = K_m \dot{\gamma}^m, \tag{13}$$

where both parameters of the consistency K_m and the power-law exponent m for $\sigma_{\Delta 1}$ scaling are also functions of the xanthan concentration.

Equations (12) and (13) can be used to fit each curve in Figs. 2(a) and 2(b) for different C_p values by applying regressions with 99% confidence. Accordingly, empirical plots are obtained as a function of C_p, as provided in Figs. 3 and 4 for η and $\sigma_{\Delta 1}$, respectively. The best curve fits for K_n and n in Fig. 3 and for K_m and m in Fig. 4 give the following empirical correlations:

$$K_n = 3.442 C_p^{1.533}; \quad n = 0.36 C_p^{-0.171}, \tag{14}$$

$$K_m = 0.296 C_p^{1.593}; \quad m = 0.752. \tag{15}$$

Therefore, the empirical viscometric functions for the shear viscosity and the first normal stress difference are

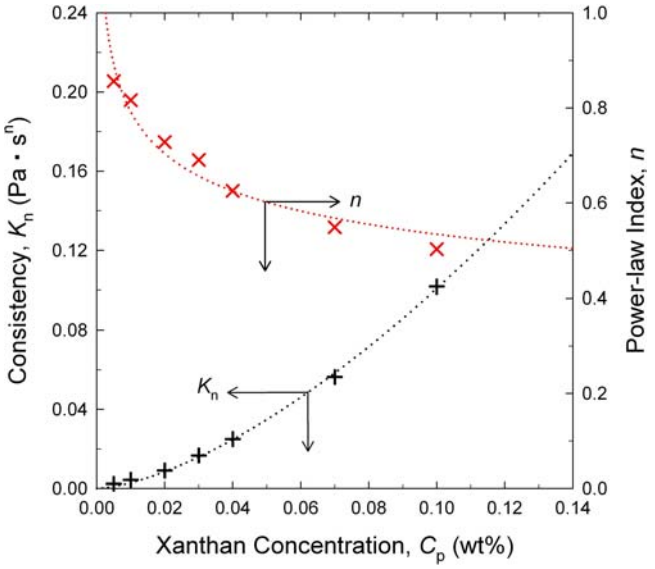

Fig. 3. (Color online) Dependence of the viscosity parameters (K_n and n) on the xanthan concentration C_p obtained by fitting for experimental data of Fig. 2(a). The dotted lines are the best fitting for K_n and n.

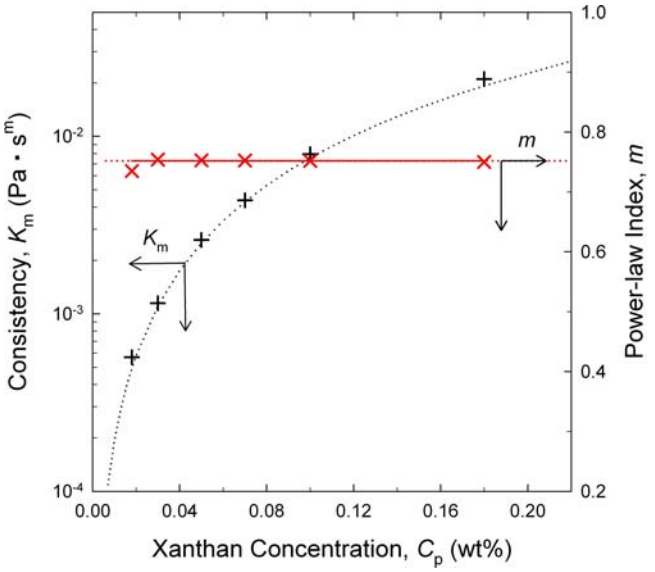

Fig. 4. (Color online) Dependence of the first normal stress difference parameters (K_m and m) on the xanthan concentration C_p obtained by fitting for experimental data of Fig. 2(b). The dotted lines are the best fitting for K_m and m.

expressed as

$$\eta = 3.442 C_p^{1.533} \dot{\gamma}^{0.36 C_p^{-0.171} - 1}, \tag{16}$$

$$\sigma_{\Delta 1} = 0.296 C_p^{1.593} \dot{\gamma}^{0.752}. \tag{17}$$

In order to check the universality of the above corrections, empirical curves for different concentrations plotted by Eqs. (16) and (17) are compared to the prescribed experimental data. In Figs. 5(a) and 5(b), the agreement is not perfect yet, but is fairly satisfactory for $\dot{\gamma} > 1\ \mathrm{s}^{-1}$,

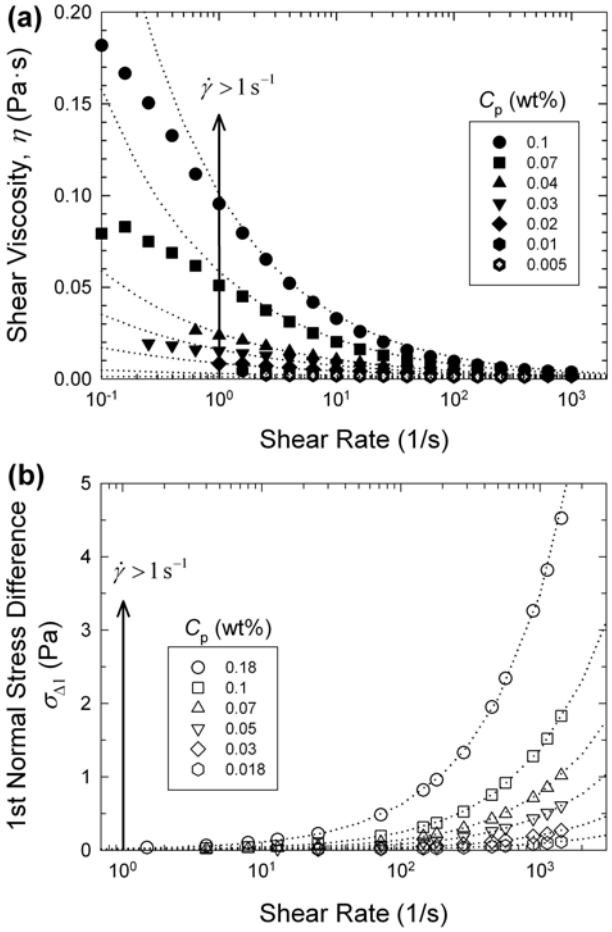

Fig. 5. Comparisons between experimental data and empirical correlations indicated by dotted curves for (a) shear viscosity and (b) first normal stress difference. Empirical curves are obtained by Eqs. (16) and (17), respectively.

indicating that the empirical correlations are applicable at dilute as well as finite concentrations of polyelectrolyte in solvents.

From Eqs. (1), (16), and (17), we ultimately construct an empirical formula for the characteristic relaxation time for xanthan, expressed as

$$\lambda(\dot{\gamma}, C_p) = 0.043 C_p^{0.06} \dot{\gamma}^{-0.248-0.36 C_p^{-0.171}}. \qquad (18)$$

As shown in Fig. 6, λ decreases with increasing shear rate, noting that the decreasing (*i.e.*, negative) slope becomes greater with decreasing xanthan concentration. C_p less than 10^{-4} wt% (*i.e.*, 1 ppm) is close to a dilute limit regime. Although Eq. (18) is restricted on the full coverage of the shear rate, agreements between the empirical η and $\sigma_{\Delta 1}$ results and their experimental data allow acquiring accurate estimates of λ for $\dot{\gamma} > 1\ \mathrm{s}^{-1}$.

The non-Newtonian fluid behavior over a full range of shear rate is available to further interpret. Rheological data presented in Fig. 2(a) possess the two asymptotes of Newtonian and shear thinning regimes. The xanthan solution shows a constant zero-shear-rate viscosity of η_0

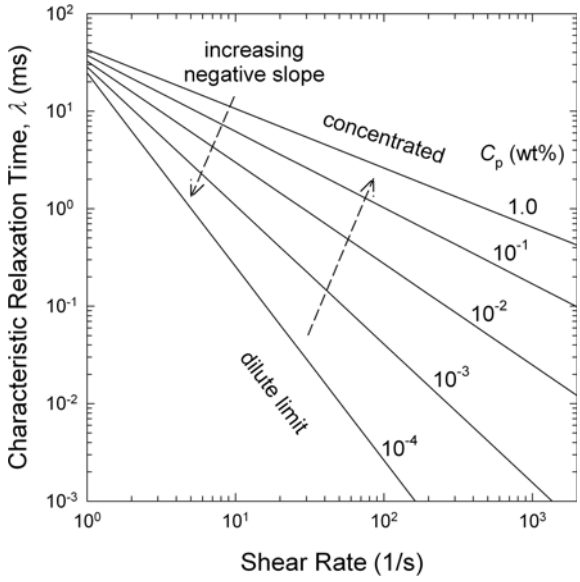

Fig. 6. Empirically determined characteristic relaxation time as functions of shear rate and xanthan concentration.

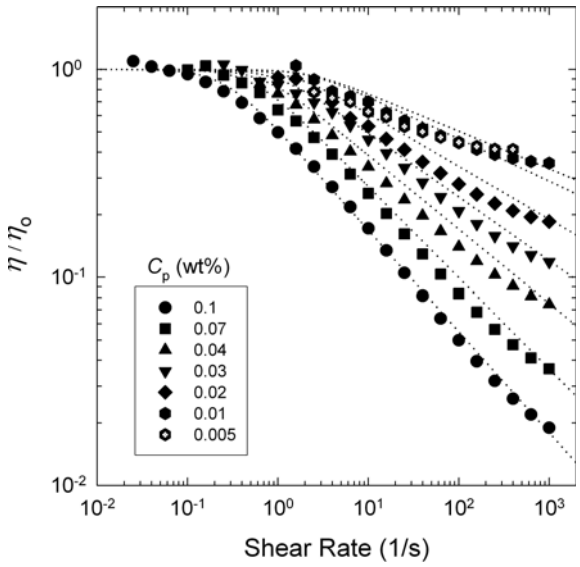

Fig. 7. Master plot of the shear viscosity after being normalized by η_0 as a function of shear rate for different xanthan concentrations. The dotted curves are the best fitting on the basis of the Carreau A model.

as $\dot{\gamma} \to 0$, whereas the viscosity decreases linearly on a log-log plot as $\dot{\gamma} \to \infty$. This can be described by the Carreau A constitutive model [27,28]

$$\eta(\dot{\gamma}, C_p) = \eta_0 \left[1 + (\lambda_T \dot{\gamma})\right]^{(n-1)/2}. \qquad (19)$$

The empirical time constant λ_T defines the critical shear rate ($\dot{\gamma}_C = 1/\lambda_T$), at which the turnover occurs between the Newtonian plateau and the shear thinning region. From the best fittings to each data for different xanthan concentrations C_p, the parameters in Eq. (19) (*i.e.*, η_o,

λ_T, and n) are determined as functions of C_p as

$$\eta_0 = -0.0167 + 0.0165e^{25.37C_p};$$
$$\lambda_T = 0.4 + 10.88C_p + 221C_p^2;$$
$$n = 0.928 - 1.29C_p^{0.483}. \quad (20)$$

In Fig. 7, the shear viscosity is normalized by its zero-shear value and is plotted versus the shear rate for different C_p. We emphasize that empirical plots for each concentration fitted by using the Carreau A model are applicable to the region of lower shear rate ($\dot{\gamma} > 1$ s^{-1}), which cannot be achieved in Fig. 5(a).

IV. CONCLUSION

Polyelectrolytes include many biopolymers, which have stimulated interest from fundamental, as well as technological, points of view. The characteristic relaxation time λ is approximately equivalent to the sum of the relaxation times for each of the normal modes of the Rouse-Zimm model. By revisiting the theory of polymer dynamics in dilute solutions, we set up each formula of the relaxation time for each model as a function of the intrinsic viscosity. For solutions beyond the dilute concentration, there are few theoretical and experimental studies readily reporting λ of a semiflexible polyelectrolyte solution, and the available results are sometimes conflicting.

We developed an empirical approach for estimating λ by means of rheological correlations. Rheological data of shear viscosity and first normal stress difference were measured for the semiflexible polyelectrolyte xanthan ranging from dilute to semidilute concentrations, and yielded power-law scaling relations for $\dot{\gamma} > 1$ s^{-1}. Empirical plots obtained by regressions on η and $\sigma_{\Delta 1}$ as functions of $\dot{\gamma}$ and C_p were used to determine each of the empirical fitting parameters. Fair agreements between empirical curves and experimental data ensure that our empirical correlations are justified to apply at dilute and finite concentrations. Subsequently, a formula for the relaxation time can be set up from the empirical viscometric functions of η and $\sigma_{\Delta 1}$. It should be pointed out that our empirical study provides insight into the dynamics of polyelectrolytes in dilute as well as finite concentrated solutions.

ACKNOWLEDGMENTS

This work was supported by the Basic Research Fund (No. 20100021979) from the National Research Foundation of Korea provided to M.-S.C. The authors acknowledge the Chemical Engineering Department at the Korea University and TA Instruments Korea for the use of rotational rheometers. S.H. Choung assisted in measuring the data.

REFERENCES

[1] K. Kremer and K. Binder, Comput. Phys. Rep. **7**, 259 (1988).
[2] C. Peter and K. Kremer, Faraday Discuss. **144**, 9 (2010).
[3] C. Holm, P. Këkicheff and R. Podgornik, *Electrostatic Effects in Soft Matter and Biophysics, NATO Science Series II: Mathematics, Physics and Chemistry* (Kluwer, Dordrecht, 2001), Vol. 46.
[4] J. Jeon and M.-S. Chun, J. Chem. Phys. **126**, 154904 (2007).
[5] N. B. Wyatt and M. W. Liberatore, Soft Matter **6**, 3346 (2010).
[6] A. Balducci, C.-C. Hsieh and P. S. Doyle, Phys. Rev. Lett. **99**, 238102 (2007).
[7] Y. Jung, S. Jun and B.-Y. Ha, Phys. Rev. E **79**, 061912 (2009).
[8] A. Milchev, J. Phys. Condens. Matter **23**, 103101 (2011).
[9] J. T. Mannion, C. H. Reccius, J. D. Cross and H. G. Craighead, Biophys. J. **90**, 4538 (2006).
[10] S. L. Levy and H. G. Craighead, Chem. Soc. Rev. **39**, 1133 (2010).
[11] E. A. Strychalski, J. Geist, M. Gaitan, L. E. Locascio and S. M. Stavis, Macromolecules **45**, 1602 (2012).
[12] M. Doi and S. F. Edwards, *The Theory of Polymer Dynamics* (Clarendon, Oxford, 1986).
[13] M. Rubinstein and R. H. Colby, *Polymer Physics* (Oxford University Press, New York, 2003).
[14] P. E. Rouse, J. Chem. Phys. **21**, 1272 (1953).
[15] B. H. Zimm, J. Chem. Phys. **24**, 269 (1956).
[16] T. T. Perkins, S. R. Quake, D. E. Smith and S. Chu, Science **264**, 822 (1994).
[17] P. G. DeGennes, Science **276**, 1999 (1997).
[18] E. S. G. Shaqfeh, J. Non-Newtonian Fluid Mech. **130**, 1 (2005).
[19] Y. Liu, Y. Jun and V. Steinberg, J. Rheol. **53**, 1069 (2009).
[20] Y. Zhang, J. J. de Pablo and M. D. Graham, J. Chem. Phys. **136**, 014901 (2012).
[21] M. Abramowitz and I. A. Stegun, *Handbook of Mathematical Functions with Formulas, Graphs, and Mathematical Tables* (Dover Publication, New York, 1972).
[22] R. J. Gordon and W. R. Schowalter, T. Soc. Rheol. **16**, 79 (1972).
[23] W. E. Rochefort and S. Middleman, J. Rheol. **31**, 337 (1987).
[24] T. A. Camesano and K. J. Wilkinson, Biomacromolecules **2**, 1184 (2001).
[25] M.-S. Chun, C. Kim and D. E. Lee, Phys. Rev. E **79**, 051919 (2009).
[26] S. Choung, M.-S. Chun and C. Kim, J. Korean Phys. Soc. **59**, 2847 (2011).
[27] G. Chauveteau, J. Rheol. **26**, 111 (1982).
[28] K. S. Sorbie, J. Colloid Interface Sci. **139**, 299 (1990).